Journal of Engineering Physics and Thermophysics, Vol. 73, No. 2, 2000

COMPARATIVE ANALYSIS OF TURBULENCE MODELS

E. P. Sukhovich

UDC 532.517.4

A comparative analysis is performed for a complete locally anisotropic turbulence model of the second order and existing turbulence models. The comparison draws on experimental data, data of a direct numerical simulation of the nonstationary Navier–Stokes equations for a developed channel flow and a uniform channel flow with a constant velocity shift, and results for turbulence damping behind a grid. The K–ε model and the quasi-isotropic turbulence model are shown to have marked disadvantages, especially in describing turbulent flows with a high degree of anisotropy of pulsatory motion. Use of a locally anisotropic turbulence model improves the accuracy of determining Reynolds stresses. Consideration is given to the advantages and disadvantages of the turbulence models discussed.

Introduction. Applied problems of hydrodynamics and heat and mass transfer in turbulent fluid flows must be solved using one or another turbulence model. A great many works have now been published that describe turbulence models of different degrees of complexity. The K–ε turbulence model is the most popular. However, in many cases use of the K–ε model for describing intricate turbulent flows does not produce results that agree with experimental data. Therefore, it is reasonable to employ a more complex turbulence model for Reynolds stresses that takes account of the anisotropy of the latter. Comparison of numerical results with reliable experimental data has revealed that the turbulence models for Reynolds stresses that have been developed to date describe the dissipation process and the process of energy redistribution between the components of the Reynolds stresses as a result of pressure pulsations with insufficient accuracy. In recent years, turbulence models have been actively worked out that take into account not only the anisotropy of the Reynolds stresses but also the anisotropy of the dissipation processes.

The current work aims at analyzing the accuracy and ranges of applicability of the above turbulence models. Consideration is given to some existing turbulence models and a complete turbulence model of the second order obtained in [8-10]. A comparison is made using experimental data for a uniform channel flow with a constant velocity shift and data for turbulence damping behind a grid. Below, a brief description of the principal turbulence models discussed in the work is given.

***K*–ε Model.** The published literature has offered a great number of various versions of the K–ε model. A review of works published before 1984 is presented in [1]. The basic equations of the model have the form

$$\frac{DK}{Dt} = P_k - \tilde{\varepsilon} + D_k ; \tag{1}$$

$$\frac{D\varepsilon}{Dt} = C_{\varepsilon 1} f_1 \frac{\varepsilon P_k}{K} - C_{\varepsilon 2} f_2 \frac{\varepsilon^2}{K} + C_\varepsilon \left(\frac{K}{\varepsilon} R_k \varepsilon_{,l} \right)_{,k} + E ; \tag{2}$$

$$b_{ij} = \frac{R_{ij}}{2K} - \frac{1}{3}\delta_{ij} = -\nu_{roman} \frac{1}{K} S_{ij} , \quad S_{ij} = \frac{1}{2}(U_{i,j} + U_{j,i}) ; \tag{3}$$

Institute of Physics of Latvian University, Salaspils, Latvia. Translated from Inzhenerno-Fizicheskii Zhurnal, Vol. 73, No. 2, pp. 328-339, March–April, 2000. Original article submitted August 7, 1998.

 1062-0125/00/7302-0318$25.00 ©2000 Kluwer Academic/Plenum Publishers

$$\nu_t = C_\mu f_\mu \frac{K^2}{\tilde{\varepsilon}}, \quad \tilde{\varepsilon} = \varepsilon - D; \tag{4}$$

$$C_\mu = 0.09, \quad C_{\varepsilon 1} = 1.45, \quad C_{\varepsilon 2} = 1.9, \quad C_\varepsilon = 0.15. \tag{5}$$

The various versions of the model differ in the form of the empirical wall functions f_μ, f_1, f_2, E, and D. A table that provides corresponding relations for these functions proposed in published works is given in [2]. It should be noted that the introduction of such a large number of wall functions indicates serious shortcomings of the model that make it impossible to calculate boundary-layer flows at the wall with an acceptable degree of accuracy. An analysis [3] demonstrated that the K–ε model can be derived from a more complex model for Reynolds stresses under the following assumptions: small-scale motions are isotropic, velocity gradients are small, and equilibrium between the generation of turbulent energy and the dissipation rate is maintained in the flow. Furthermore, the model is valid only for plane flows with a simple velocity shift. The above constraints narrow the range of applicability of the considered model so much that it is difficult in practice to find a flow for which the K–ε model can be used. However, the latter is employed in many works for calculating stratified, swirling, and other intricate flows. As a rule, in these cases, in order that calculated results agree with experimental data, various empirical functions are introduced that do not have sufficient physical substantiation.

Quasi-isotropic Turbulence Model for Reynolds Stresses. Among contemporary turbulence models, turbulence models of the second order are widely popular. A way to construct them was proposed in the early 70s in [4]. The essence of this approach lies in the fact that the Reynolds stresses should be determined from an exact equation for second single-point moments. Results of the latest investigations are published in [5]. The basic equations of the model have the form

$$\frac{DR_{ij}}{Dt} = F_{ij} + P_{ij} + \Phi_{ij} - 2\varepsilon_{ij} + D_{ij}, \tag{6}$$

$$\frac{D\varepsilon}{Dt} = C_{\varepsilon 1}\frac{\varepsilon P_k}{K} - C_{\varepsilon 2}\frac{\varepsilon^2}{K} + C_\varepsilon\left(\frac{K}{\varepsilon}R_{kl}\varepsilon_{,l}\right)_{,k}, \tag{7}$$

$$\varepsilon_{ij} = \frac{1}{3}\varepsilon\delta_{ij}, \quad D_{ij} = -C_s\left[\frac{K}{\varepsilon}R_{kl}R_{ij,l}\right]_{,k}, \tag{8}$$

$$\Phi_{ij} = -C_1\varepsilon b_{ij} +$$

$$+ 4K\left[d_1 S_{ij} + d_2\left(b_{ip}S_{pj} + b_{jp}S_{pi} - \frac{2}{3}\langle bS\rangle\delta_{ij}\right) + d_3\left(b_{ip}W_{pj} + b_{jp}W_{pi}\right)\right], \tag{9}$$

$$W_{ij} = \frac{1}{2}(U_{i,j} - U_{j,i}), \quad \langle bS\rangle = b_{ij}S_{ji} = \frac{1}{2}\frac{P_k}{K}, \quad II_b = -\frac{1}{2}b_{ik}b_{ki}, \quad C_s = 0.22; \tag{10}$$

$$C_1 = 3.4 + 1.8\frac{P_k}{\varepsilon}, \quad d_1 = 0.2 - 0.325\,(-2II_b)^{1/2}, \quad d_2 = 0.3125, \quad d_3 = 0.1. \tag{11}$$

The coefficients $C_{\varepsilon 1}$, $C_{\varepsilon 2}$, and C_ε are taken to be the same as in (5).

In [6, 7], the advantages and disadvantages of the model considered were analyzed. It was found that it permits prediction of a series of effects that cannot be described by turbulence models that use the notion of

the coefficient of turbulent viscosity. Yet, there are a number of numerical calculations that describe experimental data inadequately. According to current views, the following reasons are behind the disadvantages of the model:

1. In some cases, approximation (9) describes the energy redistribution in terms of the pressure pulsations erroneously. Simple addition of a few more empirical coefficients to the existing relation for Φ_{ij} cannot lead to a positive result. A qualitative improvement of the description of the redistribution process requires fundamentally novel approaches to the closing methodology.

2. The assumption of isotropy of the dissipation processes is not supported by existing experimental data or data of direct numerical simulation. Therefore, the relation for ε_{ij} in (8) should be recognized as inadequate. Determination of ε_{ij} from the corresponding differential equation seems more promising.

3. The most serious drawback of the turbulence model is errors linked with an incorrect description of the dissipation process. It should be noted that Eq. (7) for the dissipation rate is based on intuitive notions. A proper description of the dissipation process requires modeling of the exact equation for the dissipation rate.

Locally Anisotropic Turbulence Model of the Second Order. The exact equations for second single-point moments have the form

$$\frac{DR_{ij}}{Dt} = F_{ij} + P_{ij} + \Phi_{ij} - 2\varepsilon_{ij} + D_{ij}, \tag{12}$$

$$\frac{D\varepsilon_{ij}}{Dt} = F_{(\varepsilon)ij} + P_{(\varepsilon 1)ij} + P_{(\varepsilon 2)ij} + P_{(\varepsilon 3)ij} + P_{(\varepsilon 4)ij} + \Pi_{(\varepsilon)ij} + D_{(\varepsilon)ij} + T_{(\varepsilon)ij} - Y_{(\varepsilon)ij}. \tag{13}$$

Within the framework of the complete turbulence model of the second order, the term P_{ij} is expressed in terms of the known correlation R_{ij}, and the tensor of the dissipation rate ε_{ij} is determined from Eq. (13). The terms Φ_{ij} and D_{ij} contain higher-order correlations and, as a consequence, must be expressed in terms of known correlations. The exact equation for the tensor of the dissipation rate involves five generation terms: $F_{(\varepsilon)ij}$, $P_{(\varepsilon 1)ij}$, $P_{(\varepsilon 2)ij}$, $P_{(\varepsilon 3)ij}$, and $P_{(\varepsilon 4)ij}$, and $\Pi_{(\varepsilon)ij}$ is a correlation that determines the redistribution of the dissipation rate ε_{ij} in terms of the pressure pulsations, $Y_{(\varepsilon)ij}$ is a correlation that determines the viscous breakdown of small-scale vortices, $T_{(\varepsilon)ij}$ is the turbulent diffusion of ε_{ij}, and $D_{(\varepsilon)ij}$ is the viscous diffusion of ε_{ij}. In Eq. (13), the terms $F_{(\varepsilon)ij}$, $P_{(\varepsilon 1)ij}$, and $D_{(\varepsilon)ij}$ are expressed in terms of known correlations and therefore do not need to be modeled. The remaining terms of Eq. (13) contain higher-order correlations, for which appropriate approximations must be found.

In [8-10], a modeling technique was proposed that is based on data of a direct numerical simulation (DNS) of the nonstationary Navier–Stokes equations for a developed channel flow. As the initial approximations for the unknown correlations use is made of relations obtained previously by the method of invariant modeling. As a result of the modeling, the type of approximations for the unknown correlations was ascertained and the empirical coefficients that enter these approximations were found.

The approximation for the correlation that describes the turbulent-energy redistribution between the components R_{ij} has the form

$$\Phi_{ij} = \Phi_{(1)ij} + \Phi_{(2)ij} + \Phi_{(3)ij}, \tag{14}$$

where $\Phi_{(1)ij}$ depends only on the interaction of the velocity pulsations and reflects the tendency of the field of velocity pulsations toward an isotropic state. In [8], the term $\Phi_{(1)ij}$ was modeled, which resulted in the approximation

$$\frac{\Phi_{(1)ij}}{\varepsilon} = -C_1 b_{ij} + C_2\left(b_{ij}^2 + \frac{2}{3} II_b \delta_{ij}\right), \tag{15}$$

$$C_1 = C_{10f} + C_{11f} F_b\,,\quad C_2 = 3C_{10f}\,,\quad C_{10f} = 1.2\,,\quad C_{11f} = 4.28\,,$$

$$F_b = 1 + 9II_b + 27III_b\,.$$

The term $\Phi_{(2)ij}$ depends on the interaction of the average velocity shift with the velocity pulsations. An approximation for this correlation was obtained in [9]:

$$\frac{\Phi_{(2)ij}}{\varepsilon} = 4\frac{K}{\varepsilon}\Bigg[d_1 S_{ij} + d_2\left(b_{ip}S_{pj} + b_{jp}S_{pi} - \frac{2}{3}\langle bS\rangle\delta_{ij}\right) + d_3\,(b_{ip}W_{pj} + b_{jp}W_{pi}) +$$

$$+ d_4\,\langle bS\rangle\left(b_{ij}^2 + \frac{2}{3}II\delta_{ij}\right) + d_4\,\langle b^2S\rangle\, b_{ij} + d_5\,\langle bS\rangle\, b_{ij} +$$

$$+ d_6\left(b_{ip}^2 S_{pj} + b_{jp}^2 S_{pi} - \frac{2}{3}\langle b^2S\rangle\delta_{ij}\right) +$$

$$+ d_7\,(b_{ip}^2 W_{pj} + b_{jp}^2 W_{pi}) + d_8\,(b_{ip}W_{pq}b_{qi}^2 + b_{jp}W_{pq}b_{qi}^2)\Bigg]\,, \tag{16}$$

where

$$\langle b^2S\rangle = b_{pq}b_{qm}S_{mp}\,;$$

$$d_{10} = 0.2\,,\quad d_{11} = 1/3\,,\quad d_2 = 1/2\,,\quad d_3 = -0.3\,,\quad d_4 = 0.2\,,\quad d_5 = -1.2\,,$$

$$d_6 = 0.1\,,\quad d_7 = -0.7\,,\quad d_8 = 0\,. \tag{17}$$

The term $\Phi_{(3)ij}$ takes into account the wall effect. The DNS data unambiguously demonstrated that the approximation $\Phi_{(3)ij}/\varepsilon$ is negligible in the entire flow region up to layers in the immediate vicinity of the wall. As a consequence, in [9] it was recommended to set

$$\Phi_{(3)ij} = 0\,. \tag{18}$$

For the diffusion term D_{ij} we use the approximation written in (8). Approximations for the unknown correlations that enter Eq. (13) can be written as [10]

$$\frac{K}{\varepsilon^2}F_{(\varepsilon)ij} = -\frac{\beta\nu}{\nu + a}\frac{K}{\varepsilon^2}\,(g_i\,\varepsilon_{(\tau)j} + g_j\,\varepsilon_{(\tau)i})\,; \tag{19}$$

$$\frac{K}{\varepsilon^2}P_{(\varepsilon1)ij} = -\frac{K}{\varepsilon}\left(\frac{\varepsilon_{ik}}{\varepsilon}U_{j,k} + \frac{\varepsilon_{ik}}{\varepsilon}U_{i,k}\right),\quad \frac{K}{\varepsilon^2}P_{(\varepsilon2)ij} = \frac{\varepsilon_{ij}}{\varepsilon}\frac{P_k}{\varepsilon}\,,\quad \frac{K}{\varepsilon^2}P_{(\varepsilon3)ij} = 0\,; \tag{20}$$

$$\frac{K}{\varepsilon^2}P_{(\varepsilon4)ij} = \gamma_1 d_{ij} + \gamma_2\delta_{ij}\,,\quad \frac{K}{\varepsilon^2}Y_{(\varepsilon)ij} = \gamma_3 d_{ij} + \gamma_4\delta_{ij}\,,\quad D_{(\varepsilon)ij} = \nu\varepsilon_{ij,kk}\,; \tag{21}$$

$$\frac{K}{\varepsilon^2}T_{(\varepsilon)ij} = C_{s2}\frac{K}{\varepsilon^2}\left[\frac{K}{\varepsilon}\,(R_{km}\,\varepsilon_{ij,m} + R_{im}\,\varepsilon_{jk,m} + R_{jm}\,\varepsilon_{ik,m})\right]_{,k}\,; \tag{22}$$

$$\frac{K}{\varepsilon^2}\Pi_{(\varepsilon)ij} = \frac{K}{\varepsilon^2}\left[\alpha_{1\varepsilon}\left(\varepsilon_{ik}U_{j,k} + \varepsilon_{jk}U_{i,k} - \frac{2}{3}\varepsilon_{mn}U_{m,n}\delta_{ij}\right) + \right.$$

$$\left. + \alpha_{2\varepsilon}\left(\varepsilon_{ik}U_{k,j} + \varepsilon_{jk}U_{k,i} - \frac{2}{3}\varepsilon_{mn}U_{n,m}\delta_{ij}\right) + \alpha_{3\varepsilon}\,\varepsilon\,(U_{i,j} + U_{j,i})\right] + \gamma_5 d_{ij}\,; \tag{23}$$

$$3\gamma_2 = a_1\frac{K}{\varepsilon^2}P_{\varepsilon 1} + a_2\frac{P_k}{\varepsilon} + a_3X_1 + a_4F_b\,,\quad 3\gamma_4 = b_1\frac{K}{\varepsilon^2}P_{\varepsilon 1} + b_2\frac{P_k}{\varepsilon} + b_3X_1 + b_4F_b\,, \tag{24}$$

where $a_1 = 1.75$, $a_2 = 3.4$, $a_3 = -0.29$, $a_4 = 3.6$, $b_1 = 1.35$, $b_2 = 3$, $b_3 = -0.06$, $b_4 = 5.6$, and $C_\varepsilon = 0.15$. The remaining coefficients of approximations (20)-(23) are unknown at present.

Equations (12)-(24) represent a complete locally anisotropic turbulence model of the second order. Approximations (14)-(18) for the correlation Φ_{ij} are new. A comparison of calculations with results of direct numerical simulation on the nonstationary Navier–Stokes equations that are presented in [8, 9] revealed that the approximations discussed describe the DNS data much more accurately than relation (9). Equations for the turbulent kinetic energy and the dissipation rate are obtained by convolution of Eqs. (12) and (13) in the indices i and j:

$$\frac{DK}{Dt} = P_k - \varepsilon + D_k\,, \tag{25}$$

$$\frac{K}{\varepsilon^2}\frac{D\varepsilon}{Dt} = C_{\varepsilon 1}\frac{P_k}{\varepsilon} - C_{\varepsilon 2} + C_{\varepsilon 3}\frac{K}{\varepsilon^2}P_{\varepsilon 1} - C_{\varepsilon 4}X_1 +$$

$$+ C_\varepsilon\frac{K}{\varepsilon^2}T_\varepsilon + \frac{K}{\varepsilon^2}(F_\varepsilon + P_{\varepsilon 3} + \Pi_\varepsilon + D_\varepsilon)\,, \tag{26}$$

where $C_{\varepsilon 1} = 1.4$, $C_{\varepsilon 2} = 2F_b$, $C_{\varepsilon 3} = 1.4$, $C_{\varepsilon 4} = 0.22$, and $C_\varepsilon = 0.15$.

The terms on the right-hand sides of Eqs. (25) and (26) can be obtained by convolution of the corresponding terms of Eqs. (12) and (13):

$$D_k = -C_s\left[\frac{K}{\varepsilon}R_kK_{,l}\right]_{,k}\,,\quad F_\varepsilon = -\frac{2\beta\nu}{\nu + a}g_i\,\varepsilon_{(\tau)i}\,,$$

$$P_{\varepsilon 1} = -2\varepsilon_{ik}U_{k,i}\,,\quad P_{\varepsilon 2} = \frac{P_k\varepsilon}{K}\,,\quad P_{\varepsilon 3} = 0\,,\quad \Pi_\varepsilon = 0\,,$$

$$P_{\varepsilon 4} = 3\gamma_2\frac{\varepsilon^2}{K}\,,\quad Y_\varepsilon = 3\gamma_4\frac{\varepsilon^2}{K}\,,\quad D_\varepsilon = \nu\varepsilon_{,kk}\,,\quad T_\varepsilon = C_s\left[\frac{K}{\varepsilon}(R_{km}\,\varepsilon_{,m})\right]_{,k}\,.$$

Uniform Flow with a Constant Velocity Shift. To obtain data needed for modeling turbulence, S. Corrsin and colleagues conducted a special series of experiments for channel flow with a constant velocity shift [11-13]. A review of works on investigating uniform flows over the last 40 years is presented in [14]. All components of the tensor of Reynolds stresses, the turbulent kinetic energy, the dissipation rate, pulsation spectra, two-point correlations, and some other parameters were measured in the experiments. The experiments were carried out for different velocity gradients. Results of the investigations were checked more than once, and their reliability raises no doubts. In view of the foregoing, we use these data for testing the turbulence models considered in the present work. To this end, we apply Eq. (25) and write Eqs. (12) and (26) in the form

$$2\frac{K}{\varepsilon}\frac{Db_{ij}}{Dt} = -2b_{ij}\left(\frac{P_k}{\varepsilon} - 1 + \frac{D_k}{\varepsilon}\right) + \left(\frac{P_{ij}}{\varepsilon} - \frac{2}{3}\frac{P_k}{\varepsilon}\delta_{ij}\right) +$$

$$+ \frac{\Phi_{ij}}{\varepsilon} - 2d_{ij} + \left(\frac{D_{ij}}{\varepsilon} - \frac{2}{3}\frac{D_k}{\varepsilon}\delta_{ij}\right), \tag{27}$$

$$\frac{K}{\varepsilon^2}\frac{D\varepsilon}{Dt} = C_{\varepsilon 1}\frac{P_k}{\varepsilon} - C_{\varepsilon 2} - 2C_{\varepsilon 3}\frac{\varepsilon_{ik}}{\varepsilon}X_1 - C_{\varepsilon 4}X_1 + C_\varepsilon\frac{K}{\varepsilon^2}\left[\frac{K}{\varepsilon}(R_{km}\varepsilon_{,m})\right]_{,k} +$$

$$+ \frac{K}{\varepsilon^2}(F_\varepsilon + P_{\varepsilon 3} + \Pi_\varepsilon + D_\varepsilon), \tag{28}$$

where

$$\left(\frac{P_{ij}}{\varepsilon} - \frac{2}{3}\frac{P_k}{\varepsilon}\delta_{ij}\right) =$$

$$= -\frac{4}{3}\frac{K}{\varepsilon}S_{ij} - 2\frac{K}{\varepsilon}\left(b_{ik}S_{kj} + b_{jk}S_{ki} - \frac{2}{3}\langle bS\rangle\delta_{ij}\right) + 2\frac{K}{\varepsilon}(b_{ik}W_{jk} + b_{jk}W_{ik}).$$

In [15] it was shown that, for the experiments presented in [11-13], the convection and diffusion terms in Eq. (27) can be disregarded, i.e.,

$$\frac{K}{\varepsilon}\frac{Db_{ij}}{Dt} \approx 0, \quad D_{ij} \approx 0, \quad D_k \approx 0.$$

It follows from [10] that, for a uniform flow, the terms $P_{\varepsilon 3}$, D_ε, Π_ε, and F_ε on the right-hand side of Eq. (28) are much smaller than the remaining terms of the equation. With allowance for these evaluations, Eqs. (27) and (28) assume the following simple form:

$$2b_{ij}\left(\frac{P_k}{\varepsilon} - 1\right) - \left(\frac{P_{ij}}{\varepsilon} - \frac{2}{3}\frac{P_k}{\varepsilon}\delta_{ij}\right) - \frac{\Phi_{(1)ij}}{\varepsilon} - \frac{\Phi_{(2)ij}}{\varepsilon} + 2d_{ij} = 0, \tag{29}$$

$$\frac{K}{\varepsilon^2}\frac{D\varepsilon}{Dt} = C_{\varepsilon 1}\frac{P_k}{\varepsilon} - C_{\varepsilon 2} - 2C_{\varepsilon 3}\frac{\varepsilon_{jk}}{\varepsilon}X_1 - C_{\varepsilon 4}X_1. \tag{30}$$

To determine the Reynolds stresses, we write Eq. (29) in a Cartesian coordinate system as

$$2b_{xx}(2X_1b_{xy} + 1) - \frac{8}{3}X_1b_{xy} + \frac{\Phi_{(1)xx}}{\varepsilon} + \frac{\Phi_{(2)xx}}{\varepsilon} - 2d_{xx} = 0, \tag{31}$$

$$2b_{yy}(2X_1b_{xy} + 1) + \frac{4}{3}X_1b_{xy} + \frac{\Phi_{(1)yy}}{\varepsilon} + \frac{\Phi_{(2)yy}}{\varepsilon} - 2d_{yy} = 0, \tag{32}$$

$$2b_{xy}(2X_1b_{xy} + 1) - 2X_1\left(b_{yy} + \frac{1}{3}\right) + \frac{\Phi_{(1)xy}}{\varepsilon} + \frac{\Phi_{(2)xy}}{\varepsilon} - 2d_{xy} = 0, \tag{33}$$

where

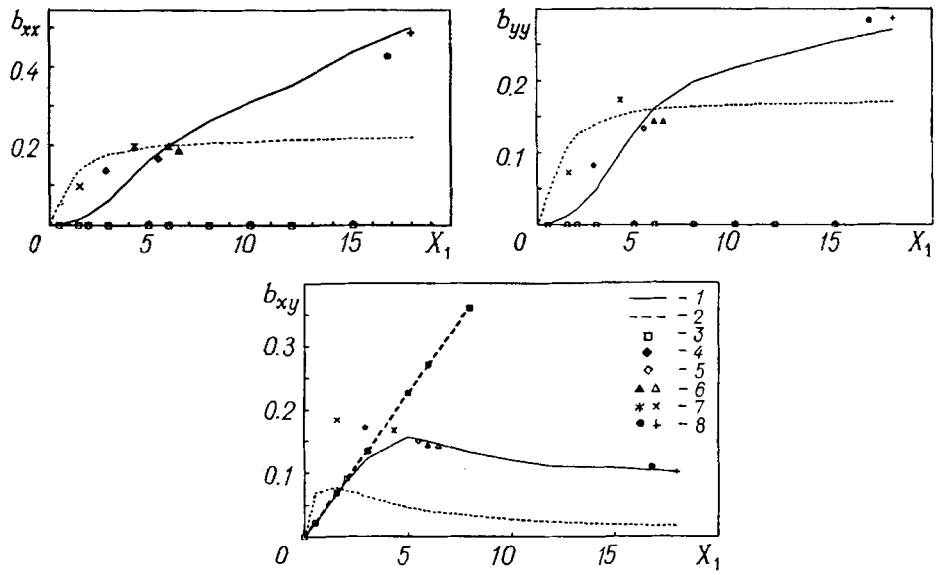

Fig. 1. Comparison of calculated results for components b_{xx}, b_{yy}, and b_{xy} of the tensor of Reynolds stresses with data for a uniform flow: 1) calculation by Eqs. (31)-(33); 2) calculation by the equations of [5]; 3) K–ε model; 4) experimental data of [12]; 5) data of [13]; 6) data of [14]; 7) DNS data of [19]; 8) DNS data of [20].

$$\frac{\Phi_{(1)xx}}{\varepsilon} = -C_1 b_{xx} + C_2\left(b_{xx}^2 + b_{xy}^2 + \frac{2}{3}II_b\right);$$

$$\frac{\Phi_{(1)yy}}{\varepsilon} = -C_1 b_{yy} + C_2\left(b_{yy}^2 + b_{xy}^2 + \frac{2}{3}II_b\right);$$

$$\frac{\Phi_{(1)xy}}{\varepsilon} = -C_1 b_{xy} + C_2 b_{xy}(b_{xx} + b_{yy});\quad II_b = -\frac{1}{2}(b_{xx}^2 + b_{yy}^2 + b_{zz}^2 + 2b_{xy}^2);$$

$$III_b = \frac{1}{3}(b_{xx}^3 + b_{yy}^3 + b_{zz}^3 + 3b_{xy}^2(b_{xx}^2 + b_{yy}^2));\quad X_1 = \frac{K}{\varepsilon}\frac{\partial U_x}{\partial y};$$

$$\frac{\Phi_{(2)xx}}{\varepsilon} = 4X_1 b_{xy}\left(\frac{1}{3}d_2 - d_3 + d_4\left(b_{xx}^2 + b_{xy}^2 + \frac{2}{3}II\right) + d_4 b_{xx} b^+ + d_5 b_{xx} + \frac{1}{3}d_6 b^+ - d_7 b^+\right);$$

$$\frac{\Phi_{(2)yy}}{\varepsilon} = 4X_1 b_{xy}\left(\frac{1}{3}d_2 + d_3 + d_4\left(b_{yy}^2 + b_{xy}^2 + \frac{2}{3}II\right) + d_4 b_{yy} b^+ + d_5 b_{yy} + \frac{1}{3}d_6 b^+ + d_7 b^+\right);$$

$$\frac{\Phi_{(2)xy}}{\varepsilon} = 2X_1(d_1 + d_2 b^+ + d_3 b^- + 4d_4 b^+ b_{xy}^2 + 2d_5 b_{xy}^2 + d_6 b_6 + d_7 b^+ b^-);$$

$$b^+ = b_{xx} + b_{yy};\quad b^- = b_{xx} - b_{yy};\quad b_6 = b_{xx}^2 + 2b_{xy}^2 + b_{yy}^2.$$

Within the framework of the complete turbulence model of the second order, the tensor of anisotropy of the dissipation rate d_{ij} must be obtained from the solution of Eq. (13). However, at present this relation cannot be used, since some coefficients of the approximations that model its correlations have not been found

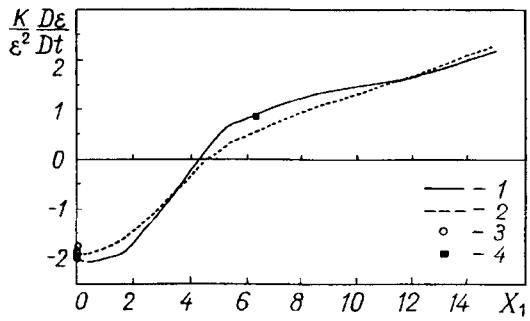

Fig. 2. Rate of variation of ε for a uniform flow: 1) calculation by Eqs. (30)-(33); 2) calculation by Eqs. (7)-(11); 3) experimental data of [17]; 4) data of [18].

as yet. In this connection, d_{ij} is determined using results of a numerical solution of the nonstationary Navier–Stokes equations for a uniform flow [16], according to which $d_{ij} \cong 0.85 b_{ij}$.

Thus, all quantities that enter Eqs. (31)-(33) have been obtained. Expressions (31)-(33) represent a nonlinear system of algebraic equations that cannot be solved in explicit form. Its analysis shows that the components of the tensor of Reynolds stresses are determined by a single dimensionless parameter X_1 that can be regarded as a local similarity parameter for a uniform channel flow with a constant velocity gradient. This system can be solved numerically. Figure 1 shows calculated results. The points in the figures represent measurement results and data of a direct numerical simulation of a uniform channel flow with a constant velocity gradient. The same figures show results calculated using the K–ε model, the quasi-isotropic turbulence model that is represented by relations (6)-(11), and the locally anisotropic model. It is seen from the figure that the K–ε turbulence model describes both the normal components of the tensor of anisotropy of the Reynolds stresses and the tangential component of this tensor inadequately. It should be noted that, in the uniform flow considered, the wall has no effect on the flow. Therefore, the large error in determining b_{xy} using the K–ε model, especially for large values of the normalized velocity gradient X_1, directly indicates substantial disadvantages of this model. Use of the quasi-isotropic turbulence model for calculations also leads to large errors in determining b_{xy}. Attention is called to the fact that the latter model has a number of modifications:

a) a complete model that presumes a solution of Eqs. (6)-(11),

b) an algebraic modification of the model that uses the Rodi hypothesis [5],

c) the same that uses a special regularization procedure [5].

In Fig. 1, the dashed lines show curves obtained by solving the complete system of equations (6)-(11).

To assess the accuracy of describing the dynamics of the variation in the dissipation rate of the turbulent kinetic energy, Fig. 2 plots $\frac{K}{\varepsilon^2}\frac{D\varepsilon}{Dt}$ vs. the normalized velocity gradient X_1. The points for $X_1 \cong 0$ indicate experimental data for turbulence damping behind a grid, published in [17], and data obtained in [18] for a uniform shear channel flow. The curves are results of calculating $\frac{K}{\varepsilon^2}\frac{D\varepsilon}{Dt}$ by Eqs. (7) and (30). It is seen from the figure that the two models for the dissipation rate are in favorable agreement with the experimental data. At the same time, the initial equations of the models considered are quite dissimiliar. Let us examine this situation in more detail. Equation (7) was modeled using experimental data for uniform turbulence. Therefore, Eq. (7) is in favorable agreement with them (see Fig. 2). In [10], results are presented from which it follows that the equation considered describes the data for a developed channel flow inadequately. Thus, the conclusion can be drawn that model equation (7) for the dissipation rate has serious disadvantages. Unlike Eq. (7), in [10] the equation for the dissipation rate was modeled on the basis of DNS data for a developed channel flow. Relation (30) thus obtained describes fairly accurately not only the data for a developed channel flow but also the data for a uniform flow that are presented in Fig. 2. Therefore, advantages of Eq. (30) over Eq. (7) can be relied

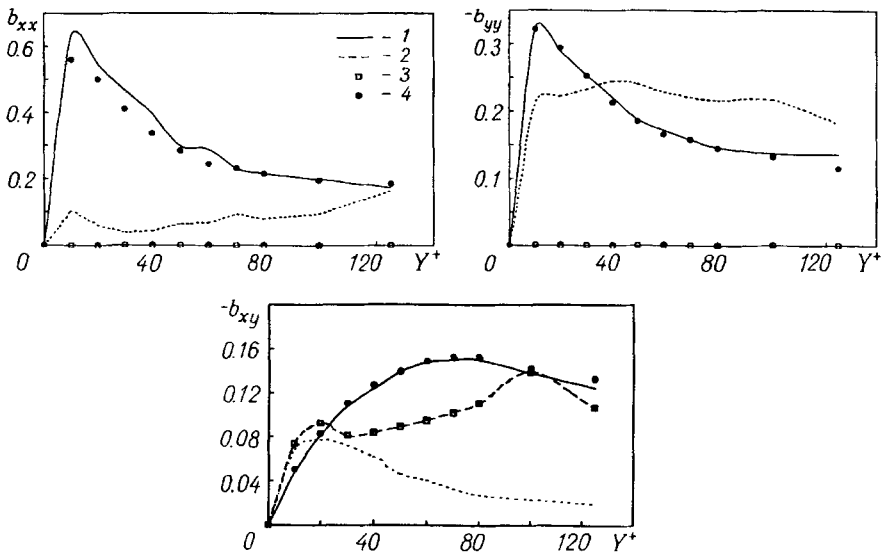

Fig. 3. Comparison of calculated results for components b_{xx}, b_{yy}, and b_{xy} of the tensor of anisotropy of Reynolds stresses with data for a developed channel flow: 1) calculation by Eqs. (31)-(33); 2) calculation by the equations of [5]; 3) K–ε model; 4) DNS data of [18].

on. A definitive conclusion as to the capabilities of Eq. (30) will permit wider testing of it using data for various flows.

Developed Channel Flow. In [18], results of a direct numerical simulation of the nonstationary Navier–Stokes equations for a developed channel flow are presented. They were employed in [8-10] for modeling unknown correlations in Eqs. (12) and (13). We use these data for testing the turbulence models considered. For a developed channel flow, $\frac{K}{\varepsilon^2}\frac{Db_{ij}}{Dt} \approx 0$, $D_{iy} \neq 0$, and $D_k \neq 0$. With allowance for these relations, the initial equation for the components of the stress tensor takes the form

$$2b_{ij}\left(\frac{P_k}{\varepsilon} - 1 + \frac{D_k}{\varepsilon}\right) + \frac{4}{3}\frac{K}{\varepsilon}S_{ij} + 2\frac{K}{\varepsilon}\left(b_{ik}S_{kj} + b_{jk}S_{ki} - \frac{2}{3}\langle bS\rangle\delta_{ij}\right) -$$

$$-2\frac{K}{\varepsilon}(b_{ik}W_{jk} + b_{jk}W_{ki}) - \frac{\Phi_{ij}}{\varepsilon} + 2d_{ij} - \left(\frac{D_{ij}}{\varepsilon} - \frac{2}{3}\frac{D_k}{\varepsilon}\delta_{ij}\right) = 0 . \qquad (34)$$

For relation (34) in a Cartesian coordinate system there is a corresponding system of nonlinear algebraic equations for the components of the tensor of anisotropy of the Reynolds stresses. It was solved using the values of the dissipation and diffusion terms from [18]. Figure 3 shows a comparison of results of solving the system of algebraic equations with data of [18]. The points in the figure show data of a direct numerical simulation that were published in [18]. The same figure presents results of calculations using the K–ε model, the quasi-isotropic turbulence model (6)-(11), and the anisotropic turbulence model of the second order. In the calculations based on the K–ε model, the wall function had the form [2]

$$f_\mu = 1 - \exp\left[-6\cdot 10^{-3}Y^+ - 4\cdot 10^{-4}(Y^+)^2 + 2.5\cdot 10^{-6}(Y^+)^3 - 4\cdot 10^{-9}(Y^+)^4\right].$$

It should be noted that good agreement between the locally anisotropic model and the DNS data is explained mainly by the fact that unknown correlations in the equation for the Reynolds stresses were modeled based on exactly these data. It is seen from the figure that the quasi-isotropic turbulence model and the K–ε turbulence

model describe both the normal components of the tensor of anisotropy of the Reynolds stresses and the tangential component of this tensor inadequately.

Discussion. Three turbulence models have been compared with available data. The models were tested using experimental data and data of a direct numerical simulation of a developed channel flow and a uniform flow with a constant velocity shift. Let us examine the main findings of testing for each of the models considered.

The best-known and most commonly used turbulence model is the K–ε model. It suggests that the turbulence anisotropy is equal to zero in all cases. The tangential component of the Reynolds stresses is determined using the notion of the coefficient of turbulent viscosity, whose magnitude is assumed from considerations of dimension to be proportional to the square of the turbulent kinetic energy and inversely proportional to the dissipation rate of the turbulent energy. The proportionality factor was selected so as to obtain the best agreement between the calculated results for the averaged characteristics and the available experimental data for a number of flows. Here, the task of describing accurately the turbulent characteristics of the flow was not undertaken. A comparison of the data for a uniform flow with a constant velocity shift with the calculations using the K–ε model revealed that the model permits determination, with an acceptable degree of accuracy, of the tangential component of the Reynolds stress at small magnitudes of the normalized velocity gradient, i.e., for $X_1 < 5$. At large magnitudes of the velocity gradient, the error becomes inadmissibly large. For a boundary-layer flow, the calculations show better agreement with the DNS data. However, an appropriate empirical wall function that ensures this agreement must be used here. Thus, the K–ε model cannot be recognized as adequate even for the two simple flows examined. This is attributable to the fact that the desire to obtain a relatively simple turbulence model has led to neglect of mechanisms essential to turbulence in constructing the K–ε model.

Unlike the K–ε model, the quasi-isotropic model is based on exact balance equations for the components of the tensor of Reynolds stresses and in this sense is fairly well justified on condition that the dissipation, diffusion, and energy redistribution between the components of the tensor of Reynolds stresses are described to sufficient accuracy. Detailed investigations [8-10] showed that the approximations for the enumerated correlations that are used in the quasi-isotropic model do not satisfy the above condition. This is explained by two reasons. First, the developers of the model sought to obtain the simplest possible approximations which would be convenient to use in subsequent numerical calculations. Second, in the years when the quasi-isotropic model was developed, there were no sufficiently detailed and reliable data for the correlation of the pressure and the strain rate or for the components of the tensor of the dissipation rate.

The results presented in the current work indicate major disadvantages of the quasi-isotropic model. The greater the velocity gradient and, correspondingly, the turbulence anisotropy, the less accurately does the model describe the data for a uniform flow with a constant velocity shift. The accuracy in describing a developed channel flow cannot be recognized as satisfactory either. It should be noted that in the current work we determined the Reynolds stresses by solving a complete nonlinear system of equations. In many published numerical calculations, a simpler algebraic modification of the quasi-isotropic model is usually employed. In this case, for calculated results to be in favorable agreement with experimental data, matching via empirical coefficients is frequently used or physically ill-founded empirical functions are introduced. Such an approach cannot be recognized as acceptable, if one seeks to devise a method of solution of turbulence problems rather than describe a specific flow.

The considered complete locally anisotropic turbulence model of the second order was obtained by modeling each of the unknown correlations in exact equations for the tensor of the Reynolds stress and the tensor of the dissipation rate. This approach yielded modeling relations that describe to good accuracy the behavior of the above correlations in flows with a high degree of turbulence anisotropy. Specifically, the approximations obtained correctly describe the behavior of the unknown correlations at all points of the boundary layer, including the immediate vicinity of the wall.

A comparison of the calculated results with the available data for a uniform flow and a channel flow demonstrated that the model adequately describes the distributions of all the components of the stress tensor

and the dynamics of the variation in the dissipation rate. Here, a single system of equations is employed for the external and internal parts of the boundary layer, and no additional empirical coefficients are introduced. The latter result must be discussed in more detail. Previously, in numerical calculations, one or another turbulence model was used for calculating just the external (turbulent) part of the boundary layer. The laminar sublayer and the transition region of the boundary layer were described using empirical relations. In this case, "joining" of these layers had to be carried out. Similar problems arose in calculations of flows with a strong anisotropy of the pulsatory motion.

As a substantial disadvantage of the model, we can note the complexity of the approximations for the correlation that determines the energy redistribution between the components of the tensor of the Reynolds stresses and the need to solve additional equations for the components of the tensor of the dissipation rate. In this connection, the question of what justifies the substantial complication of the initial equations can be brought up. The following reasoning can be produced to answer it.

To date, hundreds of works have been published that employed the K–ε model or modifications of the quasi-isotropic turbulence model. These investigations demonstrated that a single system of equations and a single system of empirical coefficients do not work in describing flows of different types. In other words, the use of relatively simple approximations for unknown correlations does not permit the development of a fairly universal turbulence model. A probable reason for this result is that the nonlinear interactions of turbulent vortices cannot be described with the aid of simple linear relations. Therefore, the complexity of the approximation by itself should raise no objections, if it describes correctly the dissipation process or the process of energy redistribution in the equation for the Reynolds stresses. Another aspect of this problem is that presently the complexity of the equations is not a serious obstacle to performing one or another numerical calculation.

In conclusion it should be noted that the proposed locally anisotropic turbulence model was tested for just two relatively simple flows. It will be possible to draw valid conclusions about the capabilities and disadvantages of the model after wider tests, including a series of numerical calculations of various flows.

NOTATION

$\frac{D}{Dt} = \frac{\partial}{\partial t} + U_k \frac{\partial}{\partial x_k}$; U_k, averaged velocity; $R_{ij} = \langle u_i u_j \rangle$, single-point correlation of velocity pulsations; $K = R_{ii}/2$, turbulent kinetic energy; $P_k = -R_{ik}U_{k,i}$, generation of turbulent energy; $\varepsilon = \nu\langle u_{i,k}u_{i,k}\rangle$, dissipation rate of Reynolds stresses; t, time; u_i, velocity pulsation; ρ, density; ν, kinematic viscosity; ν_t, coefficient of turbulent viscosity; δ_{ij}, Kronecker symbol; angular brackets denote averaging; comma in front of a subscript denotes differentiation; f_μ, f_1, f_2, E, and D, empirical wall functions; $F_{ij} = (\langle f_i u_j \rangle + \langle f_j u_i \rangle)/\rho$, term of generation of turbulent energy due to the action of the external force; $P_{ij} = -(R_{ik}U_{j,k} + R_{j,k}U_{i,k})$, generation of Reynolds stresses by the average-velocity gradient; $\Phi_{ij} = \langle p(u_{i,j} + u_{j,i})\rangle/\rho$, correlation determining energy redistribution between components R_{ij}; $\varepsilon_{ij} = \nu\langle u_{i,k}u_{j,k}\rangle$, tensor of dissipation rate; $D_{ij} = -[\langle u_i u_j u_k \rangle + (\langle \rho u_i \rangle \delta_{jk} + \langle p u_j \rangle \delta_{ik}) - \nu\langle u_i u_j \rangle_{,k}]_{,k}$, diffusion term; f_i, p, pulsations of the external force and the pressure, respectively. Correlations entering the equation for the tensor of the dissipation rate: $F_{(\varepsilon)ij} = \nu(\langle u_{i,k}f_{j,k}\rangle + (\langle u_{j,k}f_{i,k}\rangle)/\rho$, $P_{(\varepsilon 1)ij} = -(\varepsilon_{ik}U_{j,k} + \varepsilon_{jk}U_{i,k})$, $P_{(\varepsilon 2)ij} = -\nu U_{m,k}(\langle u_{i,k}u_{j,m}\rangle + \langle u_{j,k}u_{i,m}\rangle)$, $P_{(\varepsilon 4)ij} = -2\nu\langle u_{i,k}u_{j,m}u_{k,m}\rangle$, $P_{(\varepsilon 3)ij} = -\nu(\langle u_{i,k}u_m\rangle U_{j,km} + \langle u_{j,k}u_m\rangle U_{i,km})$, $Y_{(\varepsilon)ij} = -2\nu^2\langle u_{i,km}u_{j,km}\rangle$, $\Pi_{(\varepsilon)ij} = -\frac{\nu}{\rho}(\langle u_{j,k}p_{,ik}\rangle + \langle u_{i,k}p_{,jk}\rangle)$, $D_{(\varepsilon)ij} = \nu\varepsilon_{ij,kk}$, $T_{(\varepsilon)ij} = -\nu(\langle u_{i,k}u_{j,m}u_{k,m}\rangle - \varepsilon_{ij,k})_{,k}$; β, coefficient of volume expansion; g_i, acceleration due to gravity; $\varepsilon_{(\tau)i}$, dissipation term in the equation for the density of the turbulent heat flux; τ, temperature pulsation; $d_{ij} = \frac{\varepsilon_{ij}}{\varepsilon} - \frac{1}{3}\delta_{ij}$, degree of anisotropy of dissipation processes; b_{ij}, tensor of anisotropy of Reynolds stresses; II_b, III_b, and F_b, scalar invariants determining the degree of anisotropy of pulsatory motion: $II_b = -b_{ik}b_{ki}/2$, $III_b = b_{ik}b_{km}b_{mi}/3$, $F_b = 1 + 9II_b + 27III_b$, $b_{ij}^2 = b_{ik}b_{kj}$, $b_{ij}^3 = b_{ik}b_{km}b_{mj}$;

II_d, III_d, and F_d, scalar invariants determining the degree of anisotropy of dissipation processes: $II_d = -d_{ik}d_{ki}/2$, $III_d = d_{ik}d_{km}d_{mi}/3$, $F_d = 1 + 9II_d + 27III_d$; $X_1 = \frac{K}{\varepsilon}(S_{ij}S_{ij})^{1/2}$, normalized velocity gradient; $Y^+ = yu_\tau/\nu$, dimensionless distance from the wall; $u_\tau = (\nu U_{,y\,\text{wall}})^{1/2}$; $U_{,y\,\text{wall}}$, averaged-velocity gradient on the wall. The subscripts h and d indicate the way of defining scalar invariants.

REFERENCES

1. V. C. Patel, W. Rodi, and G. Scheuerer, *AIAA J.*, **23**, 1308-1319 (1985).
2. W. Rodi and N. N. Mansour, *J. Fluid Mech.*, **250**, 509-529 (1993).
3. E. P. Sukhovich, *Izv. Akad. Nauk Latv. SSR, Teplofiz. Gidrogazodinamika*, No. 1, 65-72 (1990).
4. B. E. Launder, G. J. Reece, and W. Rodi, *J. Fluid Mech.*, **68**, 537-566 (1975).
5. T. B. Gatski and C. G. Speziale, *J. Fluid Mech.*, **254**, 59-78 (1993).
6. B. E. Launder, in: A. S. Ginevskii (ed.), *Turbulent Shear Flows* [Russian translation], Vol. 1, Moscow (1982), pp. 270-279.
7. B. E. Launder and A. Morse, in: A. S. Ginevskii (ed.), *Turbulent Shear Flows* [Russian translation], Vol. 1, Moscow (1982), pp. 291-310.
8. E. P. Sukhovich, *Inzh.-Fiz. Zh.*, **72**, No. 3, 576-583 (1999).
9. E. P. Sukhovich, *Inzh.-Fiz. Zh.*, **72**, No. 4, 663-671 (1999).
10. E. P. Sukhovich, *Inzh.-Fiz. Zh.*, **72**, No. 5, 886-895 (1999).
11. S. Tavoularis and S. Corrsin, *J. Fluid Mech.*, **104**, 311-367 (1981).
12. F. H. Champagne, V. G. Harris, and S. Corrsin, *J. Fluid Mech.*, **41**, Pt. 1, 81-139 (1970).
13. V. G. Harris, J. A. Graham, and S. Corrsin, *J. Fluid Mech.*, **81**, Pt. 4, 657-687 (1977).
14. S. Tavoularis and U. Carnik, *J. Fluid Mech.*, **204**, 457-478 (1989).
15. E. P. Sukhovich, *Izv. Akad. Nauk Latv. SSR, Teplofiz. Gidrogazodinamika*, No. 3, 68-84 (1988).
16. W. J. Feiereisen, E. Scirani, J. H. Ferziger, and W. C. Reynolds, in: *Turbulent Shear Flow*, Vol. 3 (1982), pp. 309-321.
17. M. Gad-el-Hak and S. Corrsin, *J. Fluid Mech.*, **62**, Pt. 1, 115-143 (1974).
18. N. N. Mansour, J. Kim, and P. Moin, *J. Fluid Mech.*, **194**, 15-44 (1988).
19. M. M. Rogers and P. Moin, *J. Fluid Mech.*, **176**, 33-66 (1987).
20. M. J. Lee, J. Kim, and P. Moin, *J. Fluid Mech.*, **216**, 561-583 (1990).